Inflammatory chemokine receptors regulate CD8+ T cell contraction and memory generation following infection

Jacob E. Kohlmeier,[1] William W. Reiley,[1] Georgia Perona-Wright,[1] Michael L. Freeman,[1] Eric J. Yager,[2] Lisa M. Connor,[1] Erik L. Brincks,[1] Tres Cookenham,[1] Alan D. Roberts,[1] Claire E. Burkum,[1] Stewart Sell,[3] Gary M. Winslow,[3] Marcia A. Blackman,[1] Markus Mohrs,[1] and David L. Woodland[1]

[1]Trudeau Institute, Saranac Lake, NY 12983
[2]Center for Immunology and Microbial Disease, Albany Medical College, Albany, NY 12208
[3]Wadsworth Center, New York State Department of Health, Albany, NY 12201

The development of T cell memory from naive precursors is influenced by molecular cues received during T cell activation and differentiation. In this study, we describe a novel role for the chemokine receptors CCR5 and CXCR3 in regulating effector CD8+ T cell contraction and memory generation after influenza virus infection. We find that *Ccr5*$^{-/-}$ *Cxcr3*$^{-/-}$ cells show markedly decreased contraction after viral clearance, leading to the establishment of massive numbers of memory CD8+ T cells. *Ccr5*$^{-/-}$ *Cxcr3*$^{-/-}$ cells show reduced expression of CD69 in the lung during the peak of infection, which coincides with differential localization and the rapid appearance of memory precursor cells. Analysis of single chemokine receptor–deficient cells revealed that CXCR3 is primarily responsible for this phenotype, although there is also a role for CCR5 in the enhancement of T cell memory. The phenotype could be reversed by adding exogenous antigen, resulting in the activation and contraction of *Ccr5*$^{-/-}$ *Cxcr3*$^{-/-}$ cells. Similar results were observed during chronic *Mycobacterium tuberculosis* infection. Together, the data support a model of memory CD8+ T cell generation in which the chemokine-directed localization of T cells within infected tissues regulates antigen encounter and controls the extent of CD8+ T cell activation and differentiation, which ultimately regulates effector versus memory cell fate decisions.

CORRESPONDENCE
Jacob E. Kohlmeier:
jkohlmeier@trudeauinstitute.org
OR
David L. Woodland:
dwoodland@trudeauinstitute.org

Abbreviations used: BAL, bronchoalveolar lavage; FluNP, influenza nucleoprotein; MLN, mediastinal lymph node; MPEC, memory precursor effector cell; Mtb, *Mycobacterium tuberculosis*; SLEC, short-lived effector cell.

During an acute peripheral infection, antigen-bearing dendritic cells migrate to local draining lymphoid organs, where they initiate pathogen-specific T cell responses (Legge and Braciale, 2003; Allan et al., 2006). After antigen encounter, proliferation, and differentiation, effector CD8+ T cells enter the circulation and are directed to the infected site through a complex series of interactions involving adhesion molecules and chemokine receptors. Once in inflamed tissues, effector T cells follow chemotactic gradients to infected cells, and arrest their migration once they reencounter antigen to exert their effector functions on infected targets (Dustin et al., 1997; Bromley et al., 2008). After pathogen clearance, the effector CD8+ T cell pool undergoes extensive contraction, during which ~95% of pathogen-specific T cells die by apoptosis and the remaining ~5% survive to become long-lived memory cells (Williams and Bevan, 2007). The ability to skew this ratio in favor of T cell memory has broad implications for vaccinology, and therefore the signals that govern which cells are fated to undergo apoptosis and which cells will survive to persist as memory have been the subject of intense study.

Currently, a preponderance of evidence supports an important role for the inflammatory microenvironment in controlling effector versus memory cell–fate decisions (Kolumam et al., 2005; Harty and Badovinac, 2008; Prlic and Bevan, 2008; Obar and Lefrançois, 2010). Specifically, studies have shown that effector T cells

The Rockefeller University Press $30.00
J. Exp. Med. Vol. 208 No. 8 1621-1634
www.jem.org/cgi/doi/10.1084/jem.20102110

The Journal of Experimental Medicine

require inflammatory signals for their clonal expansion and differentiation, and the absence of inflammation during priming results in anergy or deletion (Badovinac et al., 2002; Redmond and Sherman, 2005; Joshi et al., 2007). However, too much inflammation, such as high levels of the proinflammatory cytokines IL-12 and IFN-γ, favors the generation of terminally differentiated effector $CD8^+$ T cells (Badovinac et al., 2005; Pearce and Shen, 2007). In contrast to inflammatory signals, homeostatic cytokines such as IL-7 and IL-15 promote the formation of memory $CD8^+$ T cells after acute infection (Schluns et al., 2000; Rubinstein et al., 2008; Sandau et al., 2010). The ability of homeostatic cytokines to enhance memory $CD8^+$ T cell formation is consistent with the idea that the IL-7Rα^{hi} effector subset present during an acute infection preferentially gives rise to long-lived memory $CD8^+$ T cells (Kaech et al., 2003; Huster et al., 2004). It should be noted, however, that enforced IL-7Rα expression does not alter the fate of terminally differentiated effector cells, suggesting that IL-7 signaling by itself is not sufficient (Hand et al., 2007). Nevertheless, it is clear that the strength and duration of the inflammatory environment can alter the ratio of IL-7Rα^{hi} memory precursor effector cells (MPECs) to IL-7Rα^{lo} short lived effector cells (SLECs), and ultimately influence the quality and magnitude of the memory $CD8^+$ T cell pool.

During influenza virus infection, effector $CD8^+$ T cells initially primed in the lung-draining lymph nodes traffic to the lung to mediate viral clearance (Kohlmeier and Woodland, 2009). Once in the lung, effector $CD8^+$ T cells are subjected to a highly inflammatory environment, and can reencounter antigen presented by local dendritic cells, infected epithelial cells, and other cells. These interactions can drive additional T cell proliferation and differentiation, which contribute to the magnitude of the effector T cell response (McGill and Legge, 2009). In addition, the interaction of effector $CD8^+$ T cells and dendritic cells in the lung promotes T cell survival via IL-15 transpresentation (McGill et al., 2010). As these studies demonstrate, antigen-specific T cells continue to receive additional instruction after arriving in the lung, but it is unclear how these instructions influence the generation of T cell memory after viral clearance.

Several chemokine receptors have been shown to play a role in the accumulation of effector T cells in the lung. CCR5 was shown to be important for the migration of circulating effector T cells into the interstitium under steady-state conditions (Galkina et al., 2005). During acute respiratory virus infection, effector T cell migration to the inflamed lung was dependent on CXCR3, with only a minor role for CCR5 (Fadel et al., 2008; Lindell et al., 2008; Kohlmeier et al., 2009). However, CCR5 does have a role in memory T cell migration to the lung airways during respiratory virus challenge, suggesting it may be important for the localization of cells to different compartments in the inflamed lung (Kohlmeier et al., 2008). Considering the role of these receptors in guiding T cells to infected sites, and the impact this may have in determining effector versus memory cell fate decisions, it is likely that chemokine receptors can influence generation of $CD8^+$ T cell memory. In the present study, we used murine models of influenza virus and *Mycobacterium tuberculosis* (Mtb) infection to investigate the role of the chemokine receptors CCR5 and CXCR3 in the generation of T cell memory. We find that *Ccr5*$^{-/-}$ *Cxcr3*$^{-/-}$ effector $CD8^+$ T cells show dramatically impaired activation within infected tissues compared with wild-type (WT) cells, resulting in attenuated contraction and greatly enhanced memory generation. The enhanced potential of virus-specific *Ccr5*$^{-/-}$ *Cxcr3*$^{-/-}$ cells to progress to memory was caused by their inability to reencounter antigen in the lung, as the addition of exogenous antigen was sufficient to induce the activation and contraction of virus-specific *Ccr5*$^{-/-}$ *Cxcr3*$^{-/-}$ T cells in the lung. These data demonstrate a novel role for inflammatory chemokine receptors in controlling effector versus memory cell fate decisions during infection.

RESULTS

Enhanced memory generation in $CD8^+$ T cells lacking both CCR5 and CXCR3

Inflammatory chemokine receptors, such as CCR5 and CXCR3, play a crucial role in directing the migration of lymphocytes to sites of inflammation. Previous studies have shown that these receptors can impact recruitment to the lung during steady-state conditions and after infection (Galkina et al., 2005; Fadel et al., 2008; Lindell et al., 2008; Kohlmeier et al., 2009). However, the role of these receptors on the generation of T cell memory after the resolution of infection has not been thoroughly addressed. One difficulty in assessing the impact of CCR5 and CXCR3 on memory T cell generation is that gene-deficient mice show different susceptibilities to influenza infection (Fig. S1). To circumvent this issue, we generated cohorts of mixed BM chimeras in which a population of T cells lacking one or both of these chemokine receptors could be directly compared with WT cells in the same animal (Fig. 1 A). After primary infection with x31 influenza, similar frequencies of influenza nucleoprotein $(FluNP)_{366\text{-}374}D^b$–specific effector $CD8^+$ T cells were elicited between WT and *Ccr5*$^{-/-}$ (Fig. 1 B), *Cxcr3*$^{-/-}$ (Fig. 1 C), or *Ccr5*$^{-/-}$ *Cxcr3*$^{-/-}$ (Fig. 1 D) T cell populations. However, 60 d after x31 infection, there was a significant difference in the frequency of $FluNP_{366\text{-}374}D^b$-specific *Cxcr3*$^{-/-}$ cells (Fig. 1 E, blue line) and *Ccr5*$^{-/-}$ *Cxcr3*$^{-/-}$ cells (Fig. 1 E, red line) compared with WT cells within the same host. This difference was greatly enhanced after secondary challenge with PR8 influenza, particularly among *Ccr5*$^{-/-}$ *Cxcr3*$^{-/-}$ cells, as the $FluNP_{366\text{-}374}D^b$-specific population accounted for nearly 40% of the total polyclonal $CD8^+$ T cell pool. Strikingly, this large $FluNP_{366\text{-}374}D^b$-specific population was maintained into secondary memory such that 20% of the total polyclonal $CD8^+$ T cell pool was specific for this epitope even at 270 d after challenge. A similar trend was observed with *Cxcr3*$^{-/-}$ cells, although the difference was not as dramatic, and *Ccr5*$^{-/-}$ cells showed no difference in the frequency of $FluNP_{366\text{-}374}D^b$-specific effector or memory $CD8^+$ T cells. Infection of intact gene-deficient mice with the less pathogenic x31 influenza virus,

which all mice survive, gave similarly enhanced memory T cell numbers compared with WT mice (Fig. S2). In addition, memory T cells generated after x31 influenza clearance were able to protect from a lethal PR8 influenza challenge, regardless of whether they lacked CCR5, CXCR3, or both chemokine receptors (Fig. S2).

To determine whether the increased number of memory T cells in *Ccr5*$^{-/-}$ *Cxcr3*$^{-/-}$ mice correlated with enhanced protection compared with WT mice, we measured viral titers of x31 influenza-immune mice after PR8 influenza challenge. As shown in Fig. 2, *Ccr5*$^{-/-}$ *Cxcr3*$^{-/-}$ mice had significantly lower viral loads than WT mice at day 2 after challenge, which is indicative of an increased number of memory T cells present in the lung in *Ccr5*$^{-/-}$ *Cxcr3*$^{-/-}$ mice at the time of challenge (Fig. 2 A). However, there was no significant difference in viral titers between WT and *Ccr5*$^{-/-}$ *Cxcr3*$^{-/-}$ mice on days 4, 6, or 8 after infection, which is consistent with the rapid recruitment of WT T cells, but not *Ccr5*$^{-/-}$ *Cxcr3*$^{-/-}$ T cells, to the lung in response to inflammation (Kohlmeier and Woodland, 2009). However, the enhanced

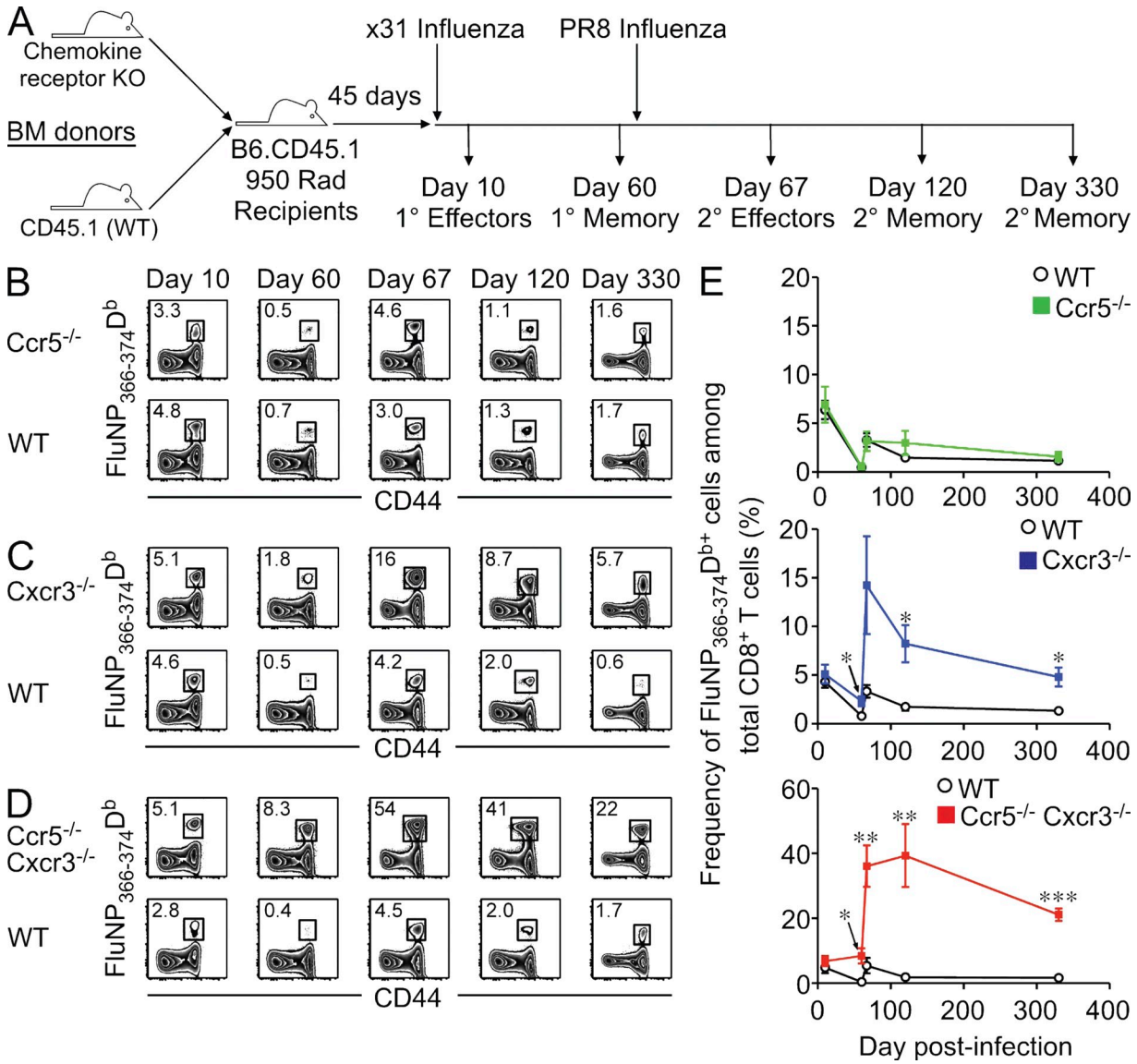

Figure 1. CD8⁺ T cells deficient in CCR5 and CXCR3 dominate the primary and secondary memory cell pool. (A) Mixed BM chimeras were generated and infected with influenza viruses as indicated to assess primary and secondary T cell responses. (B–D) Representative FluNP$_{366-374}$D^b tetramer staining from the spleen of *Ccr5*$^{-/-}$ (B), *Cxcr3*$^{-/-}$ (C), or *Ccr5*$^{-/-}$ *Cxcr3*$^{-/-}$ (D) mixed BM chimeras at the indicated times after primary and secondary influenza infection. Plots shown are gated on WT or chemokine receptor–deficient CD8⁺ T cells, and the numbers show the frequency of FluNP$_{366-374}$D^b-specific cells within that gate. (E) The frequency of FluNP$_{366-374}$D^b-specific WT (black), *Ccr5*$^{-/-}$ (green, top graph), *Cxcr3*$^{-/-}$ (blue, middle graph), or *Ccr5*$^{-/-}$ *Cxcr3*$^{-/-}$ (red, bottom graph) cells in the spleen over time (mean ± SD; *, P < 0.05; **, P < 0.005; ***, P < 0.0005). The data are representative of two independent experiments with five mice per time point.

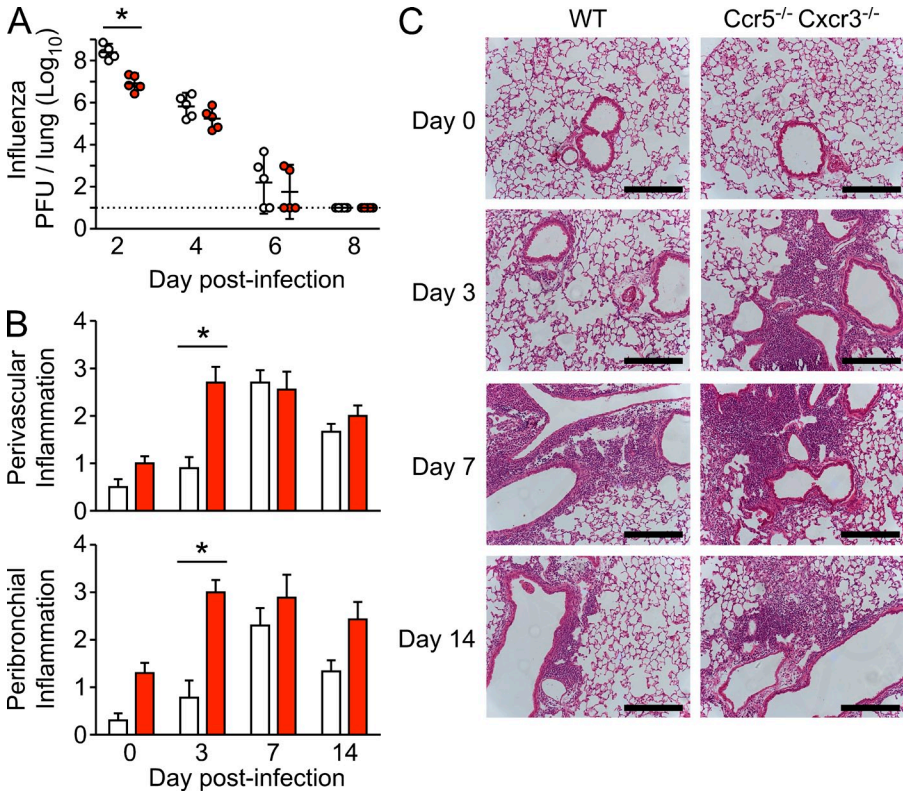

Figure 2. Increased CD8+ T cell memory in *Ccr5*$^{-/-}$ *Cxcr3*$^{-/-}$ mice results in decrease viral titers and enhanced immunopathology during the early stages of a recall response. WT and *Ccr5*$^{-/-}$ *Cxcr3*$^{-/-}$ mice were infected with 3000 EID_{50} x31 influenza virus and allowed to rest for 90 d. Mice were then challenged with 50 LD_{50} PR8 influenza virus and sacrificed at the indicated times after challenge. (A) Viral titers in the lungs of WT (open circles) and *Ccr5*$^{-/-}$ *Cxcr3*$^{-/-}$ mice (red circles) were measured at days 2, 4, 6, and 8 after challenge by plaque assay, and the dotted line indicates the limit of detection. Each symbol represents and individual mouse and the lines represent the geometric mean ± SD (*, $P < 0.05$). (B and C) Lung sections from WT (white bars) and *Ccr5*$^{-/-}$ *Cxcr3*$^{-/-}$ mice (red bars) were scored for perivascular (top graph) and peribronchial (bottom graph) inflammation on days 0, 3, 7, and 14 after challenge (mean ± SD; *, $P < 0.05$). Representative sections for WT (left column) and *Ccr5*$^{-/-}$ *Cxcr3*$^{-/-}$ mice (right column) are shown in C. Bars, 500 µm. The data are representative of 3 independent experiments with 5 mice per group (A) and 2 independent experiments with 10 mice per group (B and C).

memory T cell response in *Ccr5*$^{-/-}$ *Cxcr3*$^{-/-}$ mice was also associated with increased immunopathology during the early stage of the recall response (Fig. 2, B and C), demonstrating that there is a tradeoff between more rapid viral clearance and accelerated pathology. Together, these data show that T cells lacking CXCR3 display increased memory generation after influenza infection, and that this increase in T cell memory is greatly enhanced in cells lacking both CCR5 and CXCR3. In addition, the increased T cell memory in *Ccr5*$^{-/-}$ *Cxcr3*$^{-/-}$ mice is functional, decreasing viral loads during the early stages of a challenge infection while concomitantly resulting in more rapid immunopathology.

As the enhancement in T cell memory was most dramatic in the absence of both chemokine receptors, we chose to focus our studies on *Ccr5*$^{-/-}$ *Cxcr3*$^{-/-}$ cells. To investigate the expansion and contraction of *Ccr5*$^{-/-}$ *Cxcr3*$^{-/-}$ cells after influenza infection in greater detail, we analyzed the $FluNP_{366-374}D^b$-specific response in multiple tissues from mixed BM chimeras over time. As shown in Fig. 3 A, although the number of $FluNP_{366-374}D^b$-specific WT (black line) and *Ccr5*$^{-/-}$ *Cxcr3*$^{-/-}$ (red line) CD8$^+$ T cells is similar in many tissues at day 8 after infection, the number of *Ccr5*$^{-/-}$ *Cxcr3*$^{-/-}$ $FluNP_{366-374}D^b$-specific cells was significantly greater than the number of WT $FluNP_{366-374}D^b$-specific T cells in all tissues throughout the memory phase. Interestngly, contraction of the effector T cell pool that normally occurs after pathogen clearance was greatly impaired in *Ccr5*$^{-/-}$ *Cxcr3*$^{-/-}$ $FluNP_{366-374}D^b$-specific cells (Fig. 3 B), which explains the enhanced generation of memory. In addition, the phenotype of the *Ccr5*$^{-/-}$ *Cxcr3*$^{-/-}$ population at day 60 after infection was uniformly CD27^{hi}, CD127^{hi}, and KLRG1^{lo}, indicating that these cells are indeed resting memory cells and not merely terminally differentiated effector T cells that had survived contraction (Fig. 3 C). Furthermore, *Ccr5*$^{-/-}$ *Cxcr3*$^{-/-}$ cells show comparable cytokine and granzyme responses to WT cells during both primary and secondary responses (Fig. S3). Thus, the enhanced memory generation by cells lacking inflammatory chemokine receptors is observed in both lymphoid and nonlymphoid tissues and is caused by greatly reduced contraction after influenza infection.

Ccr5$^{-/-}$ Cxcr3$^{-/-}$ cells have limited access to antigen in the lung and decreased caspase activity

Contraction of the influenza-specific effector CD8$^+$ T cell pool typically occurs immediately after viral clearance between days 9–11 after infection (Kedzierska et al., 2006). Because we observed that *Ccr5*$^{-/-}$ *Cxcr3*$^{-/-}$ $FluNP_{366-374}D^b$-specific cells began to overtake their WT counterparts around this time (Fig. 3 A), we examined the $FluNP_{366-374}D^b$-specific population in greater detail after viral clearance. As shown in Fig. 4, A and B, whereas the frequency of WT $FluNP_{366-374}D^b$-specific cells did not change between 10–14 d after infection, the frequency of *Ccr5*$^{-/-}$ *Cxcr3*$^{-/-}$ $FluNP_{366-374}D^b$-specific cells continued to rise in all tissues after viral clearance. One explanation for this difference is that *Ccr5*$^{-/-}$ *Cxcr3*$^{-/-}$ cells continued to proliferate at a high rate after viral clearance. To test this hypothesis, we assessed BrdU incorporation in WT and *Ccr5*$^{-/-}$ *Cxcr3*$^{-/-}$ $FluNP_{366-374}D^b$-specific cells in

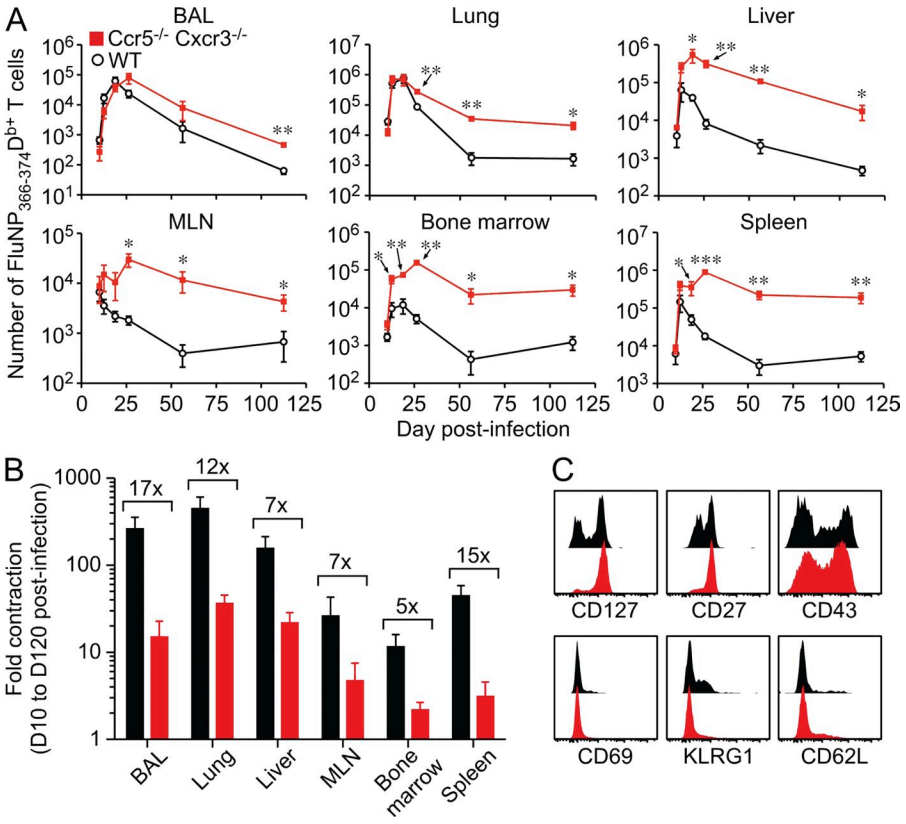

Figure 3. Increased numbers, and decreased contraction, of *Ccr5*$^{-/-}$ *Cxcr3*$^{-/-}$ T cells in all tissues after influenza infection. Mixed BM chimeras were infected with PR8 influenza virus and sacrificed at the indicated times. (A) The number of FluNP$_{366\text{-}374}$D^{b}-specific WT (black) and *Ccr5*$^{-/-}$ *Cxcr3*$^{-/-}$ (red) T cells in the indicated tissues is graphed as the mean ± SD (*, $P < 0.05$; **, $P < 0.005$; ***, $P < 0.0005$). (B) The fold contraction of WT (black) and *Ccr5*$^{-/-}$ *Cxcr3*$^{-/-}$ (red) FluNP-specific T cells comparing day 10 to day 120 after infection (mean ± SD). The numbers show the difference in fold contraction between WT and *Ccr5*$^{-/-}$ *Cxcr3*$^{-/-}$ cells. (C) The phenotype of WT (black) and *Ccr5*$^{-/-}$ *Cxcr3*$^{-/-}$ (red) memory CD8^{+} T cells on day 60 after infection. Plots are gated on FluNP$_{366\text{-}374}$D^{b+} cells and representative staining is shown. The data are representative of four independent experiments with at least five mice per time point.

the days after clearance. As expected, both populations of cells show a gradual decrease in BrdU incorporation after viral clearance (Fig. 4, C and D). However, WT cells showed equivalent, and in some cases enhanced, BrdU uptake in all tissues between days 10–14 after infection compared with *Ccr5*$^{-/-}$ *Cxcr3*$^{-/-}$ cells (Fig. 4, C and D). Thus, increased proliferation does not account for the outgrowth of *Ccr5*$^{-/-}$ *Cxcr3*$^{-/-}$ FluNP$_{366\text{-}374}$D^{b}-specific CD8^{+} T cells immediately after viral clearance.

Previous studies of T cell trafficking during respiratory virus infection have shown that CCR5 and CXCR3 play distinct, nonoverlapping roles in migration to different compartments of the lung. These findings suggest that chemokine receptor–deficient cells present in the lung during the acute phase of infection may localize to different areas than WT cells, and thus would be exposed to a different local environment and different stimuli. To test this hypothesis, we transferred equal numbers of FluNP$_{366\text{-}374}$D^{b}-specific WT and *Ccr5*$^{-/-}$, *Cxcr3*$^{-/-}$, or *Ccr5*$^{-/-}$ *Cxcr3*$^{-/-}$ memory T cells into naive congenic (CD90.1^{+} CD45.2^{+}) hosts and their localization within the lung was visualized by microscopy on day 10 after infection (Fig. 5). Around large conducting airways, where influenza virus infection and replication are commonly localized, there is a similar accumulation of WT (CD45.1^{+} CD90.2^{+}) and *Ccr5*$^{-/-}$ (CD45.1^{-} CD90.2^{+}) cells (Fig. 5 A, top row). In contrast, mice receiving a mixture of WT and *Cxcr3*$^{-/-}$ or *Ccr5*$^{-/-}$ *Cxcr3*$^{-/-}$ cells showed mostly WT cells accumulating around the large airways, with few KO cells present (Fig. 5 A, middle and bottom rows). However, examination of the interstitial spaces away from the conducting airways revealed more *Cxcr3*$^{-/-}$ and *Ccr5*$^{-/-}$ *Cxcr3*$^{-/-}$ than WT cells (Fig. 5 B). Thus, both *Cxcr3*$^{-/-}$ and *Ccr5*$^{-/-}$ *Cxcr3*$^{-/-}$ cells in the lung appear to preferentially localize in the interstitial spaces distant from the site of viral replication.

To assess whether the differential localization of WT and chemokine-receptor deficient cells in the lung resulted in these cells receiving different activation signals, we examined expression of the activation marker CD69 using mixed BM chimeras. As shown in Fig. 6 (A and B), CD69 expression in the bronchoalveolar lavage (BAL), mediastinal lymph node (MLN), and spleen was similar between WT, *Ccr5*$^{-/-}$, *Cxcr3*$^{-/-}$, and *Ccr5*$^{-/-}$ *Cxcr3*$^{-/-}$ cells. In contrast, significantly fewer *Cxcr3*$^{-/-}$ and *Ccr5*$^{-/-}$ *Cxcr3*$^{-/-}$ cells expressed CD69 compared with WT and *Ccr5*$^{-/-}$ cells in the lung, suggesting that these cells were not exposed to antigen and/or inflammation caused by differential localization within the tissue. Because we observed differential activation of WT and *Ccr5*$^{-/-}$ *Cxcr3*$^{-/-}$ cells in the lung, and activation-induced cell death is a major mechanism that contributes to T cell contraction after pathogen clearance (Strasser and Pellegrini, 2004), we investigated whether there was a differential susceptibility to apoptosis by measuring caspase activity in FluNP$_{366\text{-}374}$D^{b}-specific cells from the lung. As shown in Fig. 6 (C and D), *Ccr5*$^{-/-}$ *Cxcr3*$^{-/-}$ cells show decreased caspase activity compared with WT cells on days 10–14 after infection. Furthermore, the detectable caspase activity was largely restricted to the CD69^{+} population in both WT and *Ccr5*$^{-/-}$ *Cxcr3*$^{-/-}$ cells. Together, these data suggest that chemokine-directed localization of FluNP$_{366\text{-}374}$D^{b}-specific CD8^{+} T cells within

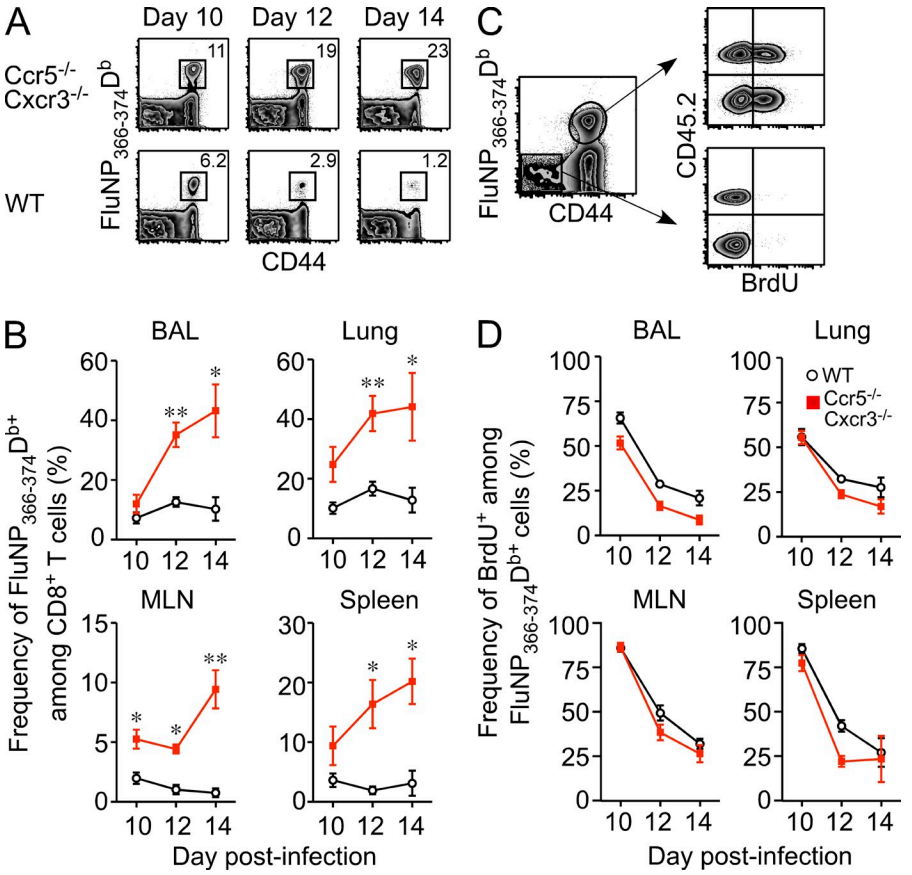

Figure 4. The rapid outgrowth of *Ccr5*$^{-/-}$ *Cxcr3*$^{-/-}$ FluNP-specific CD8$^+$ T cells after viral clearance is not caused by enhanced proliferation. Mixed BM chimeras were infected with PR8 influenza virus and sacrificed at the indicated times after infection. (A) Representative FluNP$_{366\text{-}374}$D^b tetramer staining in the spleen for *Ccr5*$^{-/-}$ *Cxcr3*$^{-/-}$ (top row) and WT (bottom row) cells on days 10, 12, and 14 after infection. Plots are gated on CD8$^+$ T cells. (B) The frequency of WT (black) and *Ccr5*$^{-/-}$ *Cxcr3*$^{-/-}$ (red) FluNP-specific cells among CD8$^+$ T cells in the BAL, lung, MLN, and spleen is graphed as the mean ± SD (*, $P < 0.05$; **, $P < 0.005$). (C) Representative staining of BrdU uptake in WT and *Ccr5*$^{-/-}$ *Cxcr3*$^{-/-}$ cells in the lung on day 12 after infection. (D) The frequency of BrdU$^+$ cells among WT (black) or *Ccr5*$^{-/-}$ *Cxcr3*$^{-/-}$ (red) FluNP-specific cells in the BAL, lung, MLN, and spleen (mean ± SD). The data are representative of three independent experiments with at least four mice per time point.

the lung parenchyma dictates which cells are able to reencounter antigen, which influences activation-induced cell death and regulates antigen-specific T cell contraction after pathogen clearance.

During acute infection, expression patterns of the IL-7Rα chain, CD127, and KLRG-1 identifies pathogen-specific CD8$^+$ T cells that preferentially survive to become long-lived memory T cells (Kaech et al., 2003). To investigate whether the chemokine receptor–deficient FluNP$_{366\text{-}374}$D^b-specific populations contained increased numbers of memory precursors compared with the WT population, we used mixed BM chimeras to analyze CD127 and KLRG-1 expression in multiple tissues. As shown in Fig. 6, although CD127 expression on FluNP$_{366\text{-}374}$D^b-specific cells was similar between WT and chemokine receptor–deficient cells at day 10 after infection, there was a significant increase in frequency of CD127$^+$ FluNP$_{366\text{-}374}$D^b-specific *Cxcr3*$^{-/-}$ and *Ccr5*$^{-/-}$ *Cxcr3*$^{-/-}$ cells compared with WT and *Ccr5*$^{-/-}$ cells by day 15 after infection. Furthermore, the difference in CD127 expression occurred almost immediately after clearance, and even in an inflamed site such as the lung (Fig. 6, E and F). Thus, after viral clearance, both *Cxcr3*$^{-/-}$ and *Ccr5*$^{-/-}$ *Cxcr3*$^{-/-}$ cells rapidly progress to MPEC phenotype, as shown by significantly increased CD127 expression, which is consistent with attenuated contraction and enhanced memory.

Chemokine receptors influence the activation and contraction of influenza-specific T cells in the lung by regulating reencounter with antigen

The decreased activation and differential localization of *Ccr5*$^{-/-}$ *Cxcr3*$^{-/-}$ cells in the lung compared with WT cells was consistent with the idea that *Ccr5*$^{-/-}$ *Cxcr3*$^{-/-}$ cells were unable to reencounter antigen in the lung and thus failed to contract after viral clearance. To test this idea, we devised an approach to force *Ccr5*$^{-/-}$ *Cxcr3*$^{-/-}$ cells to recognize their cognate antigen by repeated injections of antigen-bearing DCs (Fig. 7 A; FluNP). As a control, we injected the same DCs into a parallel cohort of mice, except these DCs had been pulsed with an irrelevant antigen (p79). As shown in Fig. 7 (B and C), injection of FluNP-pulsed DCs resulted in significantly increased CD69 expression on *Ccr5*$^{-/-}$ *Cxcr3*$^{-/-}$ cells in the lung, whereas p79-pulsed DCs had no effect. Importantly, 45 d after infection, mice that had received FluNP-pulsed DCs had a decreased frequency of influenza-specific *Ccr5*$^{-/-}$ *Cxcr3*$^{-/-}$ T cells compared with mice that had received p79-pulsed DCs (Fig. 7 D). This difference correlated with a significant decrease in the number of FluNP$_{366\text{-}374}$D^b-specific *Ccr5*$^{-/-}$ *Cxcr3*$^{-/-}$ T cells in both the lung and spleen in mice that had received FluNP-pulsed DCs (Fig. 7 E). Collectively, these data show that the addition of excess antigen leads to the activation, contraction, and decreased memory generation of *Ccr5*$^{-/-}$ *Cxcr3*$^{-/-}$ CD8$^+$ T cells. Therefore, chemokine receptors influence the generation of T cell memory after respiratory infection by controlling cellular localization and antigen reencounter in the lung, thereby altering effector versus memory cell–fate decisions.

Preferential expansion of Ccr5$^{-/-}$ Cxcr3$^{-/-}$ cells during chronic Mtb infection

Chronic infections, which are often characterized by persistent inflammation and antigen expression, have a profound effect on the accumulation and functionality on the pathogen-specific CD8$^+$ T cell pool (Shin and Wherry, 2007). For example, in patients with active Mtb infection, the pathogen-specific CD8$^+$ T cell pool is dominated by effector cells expressing a terminally differentiated phenotype (Jacobsen et al., 2007; Jurado et al., 2008). We questioned whether, even during chronic infection, *Ccr5*$^{-/-}$ *Cxcr3*$^{-/-}$ cells would be much less prone to terminal differentiation and exhaustion caused by decreased migration to inflamed areas. To test this hypothesis, we tracked the CD8$^+$ T cell response to a dominant Mtb epitope over time in mixed BM chimeras (Fig. 8). During the early stages of infection, similar frequencies of WT and *Ccr5*$^{-/-}$ *Cxcr3*$^{-/-}$ Mtb10.4$_{4\text{-}11}$K^b-specific cells were observed in the lung (Fig. 8 A), MLN (Fig. 8 B), and spleen (Fig. 8 C). However, the Mtb10.4$_{4\text{-}11}$K^b-specific population was gradually skewed in favor of *Ccr5*$^{-/-}$ *Cxcr3*$^{-/-}$ cells as the infection progressed (Fig. 8 D). Notably, the preferential accumulation of *Ccr5*$^{-/-}$ *Cxcr3*$^{-/-}$ cells occurred after day 30 of infection, after which bacterial levels stabilize and chronic infection is maintained at relatively constant level (Flynn, 2006). Therefore, even in a situation where antigen and inflammation persist, the Mtb10.4$_{4\text{-}11}$K^b-specific CD8$^+$ T cell pool becomes increasingly dominated by *Ccr5*$^{-/-}$ *Cxcr3*$^{-/-}$ cells over time.

One explanation to account for the outgrowth of *Ccr5*$^{-/-}$ *Cxcr3*$^{-/-}$ cells during chronic infection is that the inability of these cells to properly migrate limits their exposure to inflammation and antigen, which prevents or slows their terminal

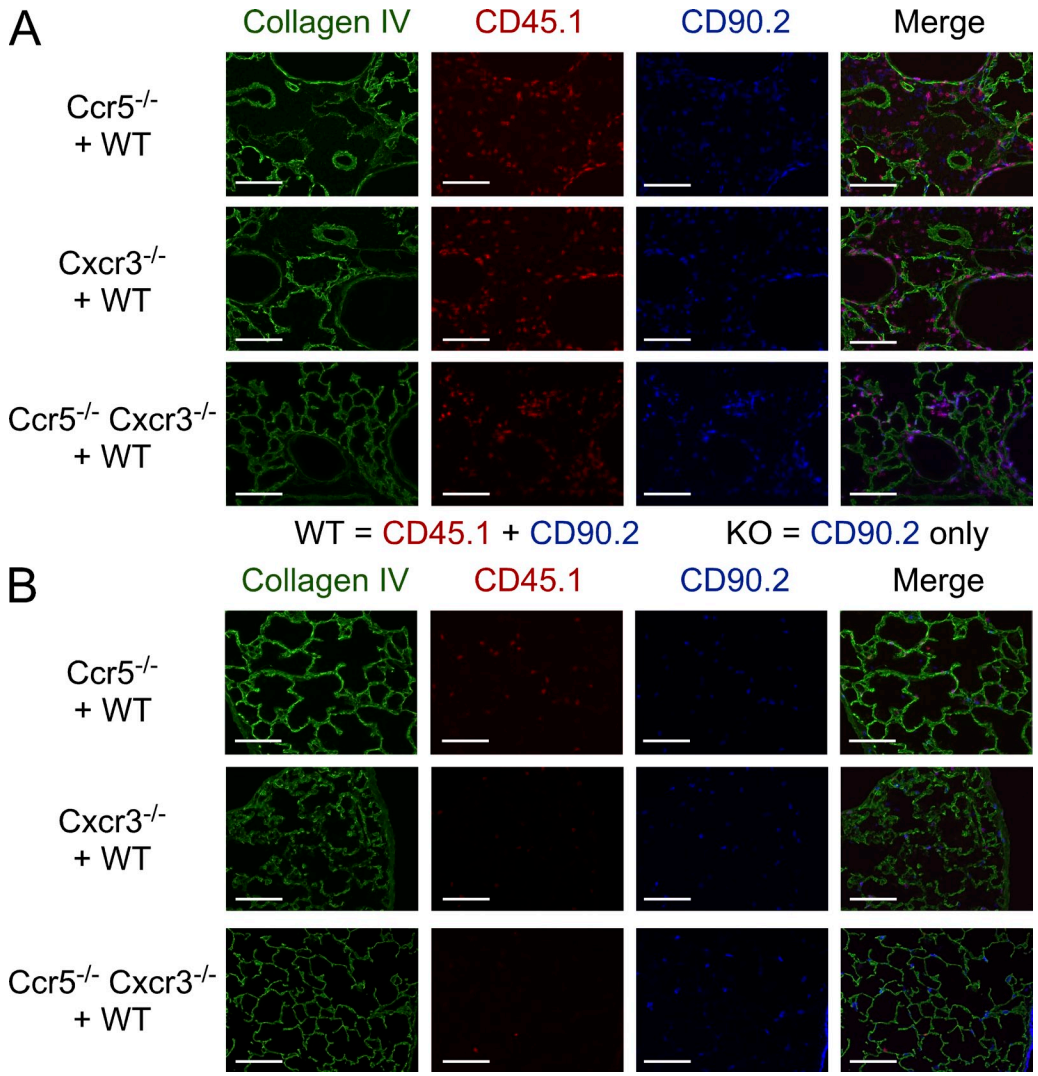

Figure 5. Differential localization of *Cxcr3*$^{-/-}$ and *Ccr5*$^{-/-}$ *Cxcr3*$^{-/-}$ cells in the lung. The localization of WT (CD45.1$^+$ CD90.2$^+$) and *Ccr5*$^{-/-}$ (CD45.1$^-$ CD90.2$^+$) cells (top row), WT and *Cxcr3*$^{-/-}$ cells (middle row), and WT and *Ccr5*$^{-/-}$ *Cxcr3*$^{-/-}$ cells (bottom row) around large conducting airways (A) or in the interstitium (B) on day 10 of an influenza infection. Collagen IV staining is shown to visualize lung morphology. Bars, 100 µm. The data are representative of three independent experiments with at least four mice per group.

differentiation. To address this possibility, we examined expression of the activation markers CD69 and CD127 on Mtb10.4_{4-11}K^b-specific WT and *Ccr5*$^{-/-}$ *Cxcr3*$^{-/-}$ cells over time. As shown in Fig. 9 (A and B), significantly fewer *Ccr5*$^{-/-}$ *Cxcr3*$^{-/-}$ cells expressed CD69 compared with WT cells in all tissues examined, and this difference became greater as the infection progressed. Strikingly, and similar to influenza infection, decreased expression of the acute activation marker CD69 correlated with increased expression of CD127 even at late times during chronic infection (Fig. 9, C and D). Thus, *Ccr5*$^{-/-}$ *Cxcr3*$^{-/-}$ Mtb10.4_{4-11}K^b-specific CD8$^+$ T cells showed limited activation caused by antigen and/or inflammation, which protected these cells from terminal differentiation and enabled their accumulation even during a chronic infection.

DISCUSSION

Chemokine receptors have been shown to play an important role in many inflammatory situations, primarily through their role in directing cellular migration. Recent studies have

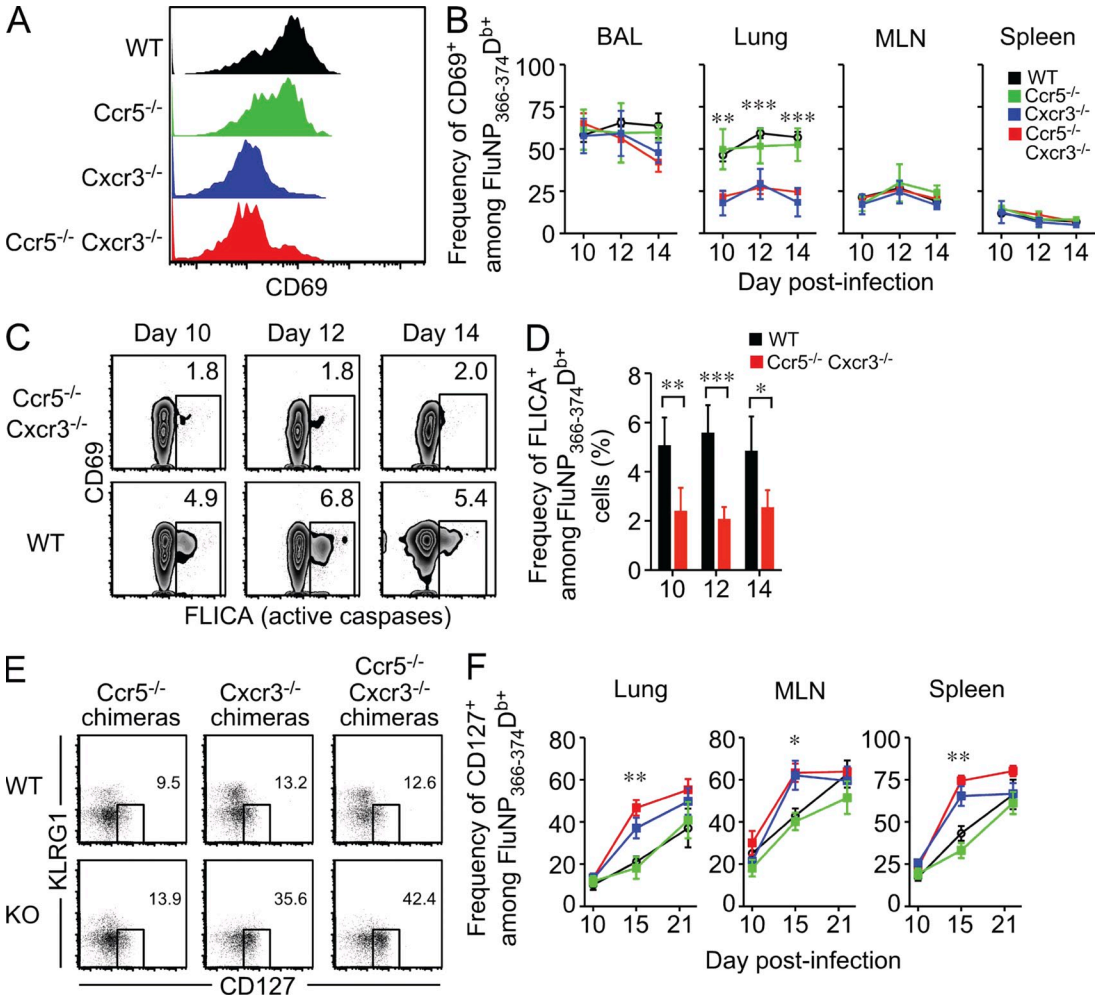

Figure 6. Decreased activation of *Cxcr3*$^{-/-}$ and *Ccr5*$^{-/-}$ *Cxcr3*$^{-/-}$ FluNP-specific cells in the lung compared with WT and *Ccr5*$^{-/-}$ cells correlates with the rapid appearance of CD127^{hi} memory precursor cells. Mixed BM chimeras were infected with PR8 influenza virus and sacrificed at the indicated times. (A) The expression of CD69 on WT (black), *Ccr5*$^{-/-}$ (green), *Cxcr3*$^{-/-}$ (blue), and *Ccr5*$^{-/-}$ *Cxcr3*$^{-/-}$ (red) FluNP-specific cells was measured by flow cytometry. The histograms show representative staining gated in FluNP$_{366-374}$D^{b+} CD8$^+$ T cells. (B) The frequency of CD69$^+$ cells among FluNP-specific CD8$^+$ T cells in the BAL, lung, MLN, and spleen on days 10, 12, and 14 after infection (mean ± SD; **, $P < 0.005$; ***, $P < 0.0005$). The WT data shown are from the WT × *Ccr5*$^{-/-}$ *Cxcr3*$^{-/-}$ mixed BM chimera, and similar data were obtained from WT in the other chimeras. (C) Representative staining of pan-caspase activity in *Ccr5*$^{-/-}$ *Cxcr3*$^{-/-}$ (top row) and WT (bottom row) FluNP-specific CD8$^+$ T cells from the lung after a 1-h incubation in vitro. The data are gated on FluNP$_{366-374}$D^{b+} cells and plotted versus CD69. (D) The frequency of FLICA$^+$ WT (black) or *Ccr5*$^{-/-}$ *Cxcr3*$^{-/-}$ (red) FluNP-specific cells in the lung on days 10, 12, and 14 after infection (mean ± SD; *, $P < 0.05$; **, $P < 0.005$; ***, $P < 0.0005$). (E) Representative staining of CD127 versus KLRG1 on WT and KO cells from various mixed BM chimeras. Staining is shown gated on FluNP$_{366-374}$D^{b+} CD8$^+$ T cells in the lung on day 15 after infection. (F) The frequency of CD127$^+$ cells among WT, *Ccr5*$^{-/-}$, *Cxcr3*$^{-/-}$, or *Ccr5*$^{-/-}$ *Cxcr3*$^{-/-}$ FluNP-specific CD8$^+$ T cells in the indicated tissues on days 10, 15, and 21 after infection (mean ± SD; *, $P < 0.05$, **; $P < 0.005$; ***, $P < 0.0005$). The data are representative of three independent experiments with at least four mice per time point.

shown that the localization of CD8$^+$ T cells to distinct microenvironments during infection can have a dramatic impact on their differentiation and ultimately determine effector versus memory T cell fate (D'Cruz et al., 2009). In this study, we demonstrate that chemokine receptor–directed localization of effector T cells within infected tissues had a profound impact on their activation state and their ability to progress onto memory. After influenza virus infection, antigen-specific CD8$^+$ T cells in the lung that lacked the inflammatory chemokine receptors CCR5 and CXCR3 showed decreased activation, were protected from apoptosis, and were largely resistant to contraction, leading to the generation of massive amounts of CD8$^+$ T cell memory. This phenotype was primarily dependent on CXCR3, although there was a role for CCR5 in the enhancement of T cell memory. These findings illustrate a new role for inflammatory chemokine receptors in regulating T cell memory generation through their control of T cell localization within infected tissues.

Many studies have focused on deciphering the signals that promote the generation of T cell memory after infection or vaccination. Signals that have the potential to influence cell fate decisions act at nearly every step of T cell activation, from initial TCR triggering and cell division to environmental signals received after pathogen clearance.

These efforts have led to the development of several models to describe the cell fate decisions that control effector versus memory commitment (Kaech and Wherry, 2007). One model in particular, which posits that the commitment

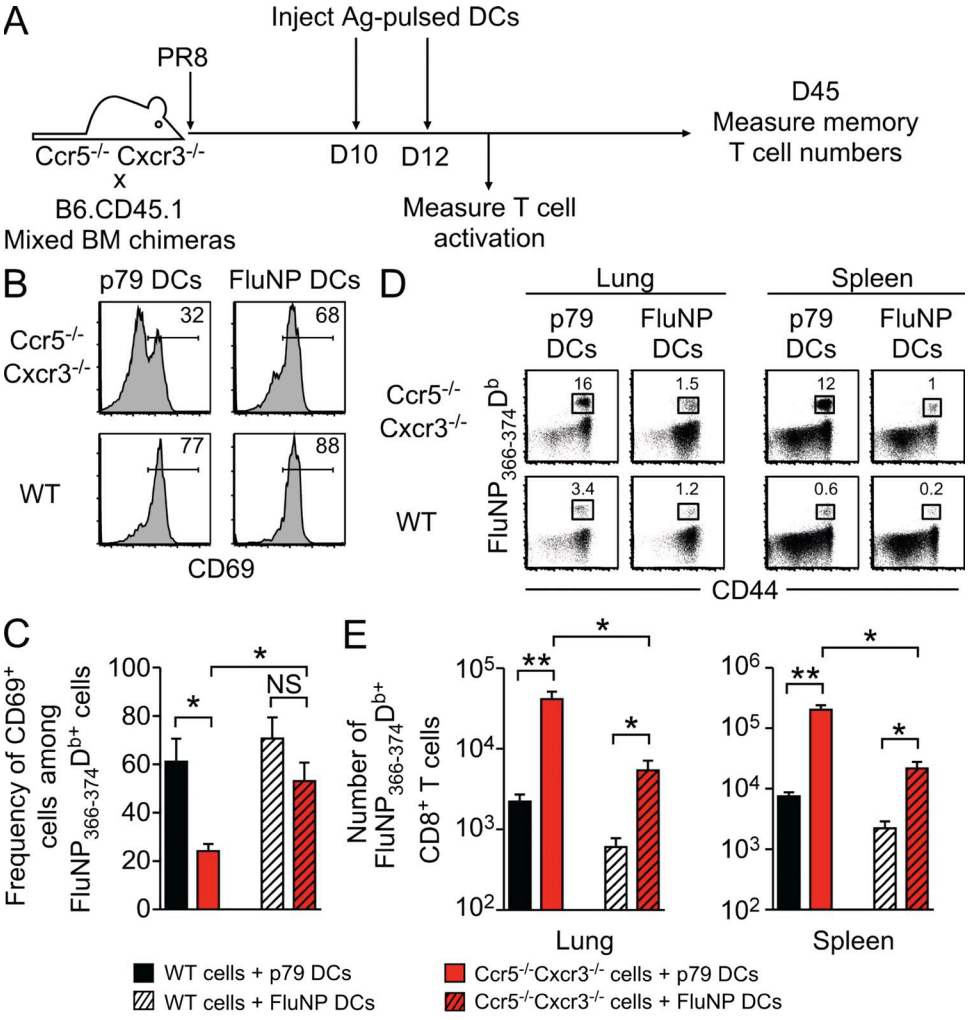

Figure 7. Cognate antigen encounter is sufficient to induce the activation of *Ccr5*$^{-/-}$ *Cxcr3*$^{-/-}$ T cells in the lung and lead to the contraction of FluNP-specific cells. (A) Mixed BM chimeras were infected with PR8 influenza virus and injected i.v. with 2 × 10^6 DCs pulsed with cognate (FluNP) or irrelevant (γHV p79) peptide on days 10 and 12 after infection. (B) Representative staining of CD69 on *Ccr5*$^{-/-}$ *Cxcr3*$^{-/-}$ (top row) and WT (bottom row) FluNP-specific cells in the lung on day 13 after infection, after transfer of p79- or FluNP-pulsed DCs. (C) The frequency of CD69$^+$ cells after DC transfer is graphed as the mean ± SD (*, $P < 0.05$). (D) Representative FluNP$_{366\text{-}374}$D^b tetramer staining of *Ccr5*$^{-/-}$ *Cxcr3*$^{-/-}$ (top row) and WT (bottom row) cells from the lung and spleen on day 45 after infection (33 d after the last DC transfer). Plots are gated on CD8$^+$ T cells. (E) The number of FluNP-specific WT (black) and *Ccr5*$^{-/-}$ *Cxcr3*$^{-/-}$ (red) T cells in the lung and spleen at day 45 after infection (the mean ± SD; *, $P < 0.05$; **, $P < 0.005$). The data are representative of two independent experiments with at least five mice per group.

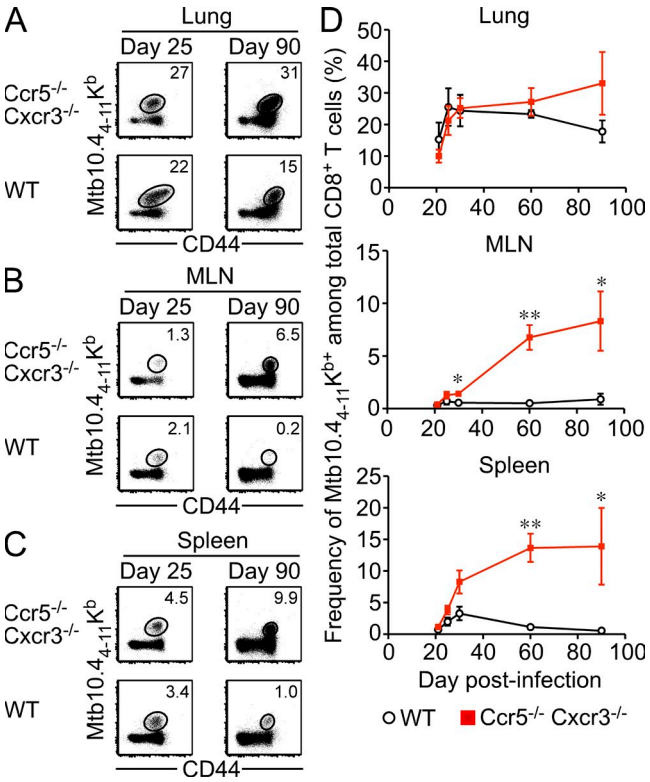

Figure 8. *Ccr5*$^{-/-}$ *Cxcr3*$^{-/-}$ cells dominate the antigen-specific response even during chronic Mtb infection. Mixed BM chimeras were infected with Mtb via the aerosol route and sacrificed at the indicated times. (A–C) Representative staining of Mtb10.4$_{4-11}$K^b tetramer on *Ccr5*$^{-/-}$ *Cxcr3*$^{-/-}$ (top row) and WT (bottom row) cells from the lung (A), MLN (B), and spleen (C) on day 25 or 90 after infection. Plots are gated on CD8$^+$ T cells. (D) The frequency of WT (black) or *Ccr5*$^{-/-}$ *Cxcr3*$^{-/-}$ (red) Mtb-specific CD8$^+$ T cells in the lung, MLN, and spleen at the indicated times after infection (mean ± SD; *, $P < 0.05$; **, $P < 0.005$). The data are representative of two independent experiments with at least four mice per group.

of cells to an effector or memory T cell fate is initially programmed at an early stage of differentiation but can be subsequently altered if additional stimuli (antigen or inflammation) are encountered, fits nicely with our data. After initial antigen encounter in the lung-draining lymph nodes, CD69–S_1P_1 interactions keep activated cells from leaving the lymph node until a sufficient number of cell divisions have occurred (Lawrence and Braciale, 2004; Shiow et al., 2006). Our data show no difference in this initial response between WT and *Ccr5*$^{-/-}$ *Cxcr3*$^{-/-}$ cells, as we observe no difference in the number of FluNP-specific cells, or in expression of CD69, within the lymph nodes during the early stages of influenza virus infection (Fig. 3 A and Fig. 6 B). However, after migration through the circulation and into the lung, we observe a dramatic difference in the activation of WT and *Ccr5*$^{-/-}$ *Cxcr3*$^{-/-}$ FluNP-specific cells, which correlates with a difference in apoptosis and memory generation. These data are consistent with the aforementioned model of differentiation, where additional encounters with antigen and/or inflammatory stimuli push antigen-specific T cells to a terminally differentiated state.

A recent study has highlighted the importance of cellular localization in controlling access to these signals, as cells with a terminally differentiated phenotype were localized to a different area of the spleen than cells with a memory precursor phenotype after LCMV infection (Jung et al., 2010). Our data suggest a model where, after initial priming and proliferation in the draining lymph nodes, effector T cells migrate to the lung, where they reencounter antigen and undergo further differentiation. Unlike WT cells, which follow chemotactic gradients to the inflamed site, *Cxcr3*$^{-/-}$ or *Ccr5*$^{-/-}$ *Cxcr3*$^{-/-}$ cells are preferentially localized to the interstitial spaces away from the primary sites of viral replication (respiratory epithelial cells lining the large airways), and the lack of additional stimuli promotes the progression of these cells into memory. However, we can artificially induce the activation and contraction of chemokine receptor–deficient cells through the addition of excess antigen, thereby forcing these cells to recognize antigen regardless of their localization. Thus, antigen reencounter in the lung controls effector versus memory cell fate decisions during influenza virus infection, and access to this antigen in the lung is regulated by chemokine-mediated cell trafficking. It should be noted that there may be additional antigen-independent signals that *Cxcr3*$^{-/-}$ or *Ccr5*$^{-/-}$ *Cxcr3*$^{-/-}$ cells fail to receive because of improper localization during initial priming in lymphoid tissues. Indeed, the accompanying article by Kurachi et al. in this issue of the *JEM* shows that CXCR3 regulates T cell fate decisions during systemic infection by regulating the proximity of T cells to inflammatory cytokines during the early expansion phase. Together, these studies suggest that CXCR3-mediated trafficking may influence T cell memory generation at multiple stages of the adaptive immune response, and raise the possibility that the primary mechanisms by which CXCR3 regulates T cell fate (i.e., access to antigen and/or inflammation) may depend on whether the host is responding to a localized versus systemic infection.

A role for inflammatory chemokine receptors in promoting initial CD8$^+$ T cell priming has been recently demonstrated. Within the lymph node, chemokine secretion by activated dendritic cells can attract CD8$^+$ T cells in a CCR5- or CCR4-dependent manner to promote T cell–dendritic cell contacts (Castellino et al., 2006; Semmling et al., 2010). In addition, several studies have noted a role for chemokine receptor–mediated signals in augmenting T cell activation irrespective of their role in T cell migration. CXCR3 ligands have been shown to enhance T cell receptor signaling during priming and induce mammalian target of rapamycin (mTOR) activation (Newton et al., 2009; Rosenblum et al., 2010; Schwarz et al., 2009). Based on these data, it is possible that certain chemokine receptor–dependent signals not being received by *Cxcr3*$^{-/-}$ or *Ccr5*$^{-/-}$ *Cxcr3*$^{-/-}$ cells during priming may influence the progression of these cells to memory. However, if this were true, the decreased activation (as measured by CD69 expression) of *Cxcr3*$^{-/-}$ and *Ccr5*$^{-/-}$ *Cxcr3*$^{-/-}$ cells compared with WT cells would be observed in all tissues. Instead, we only observe decreased CD69 expression in

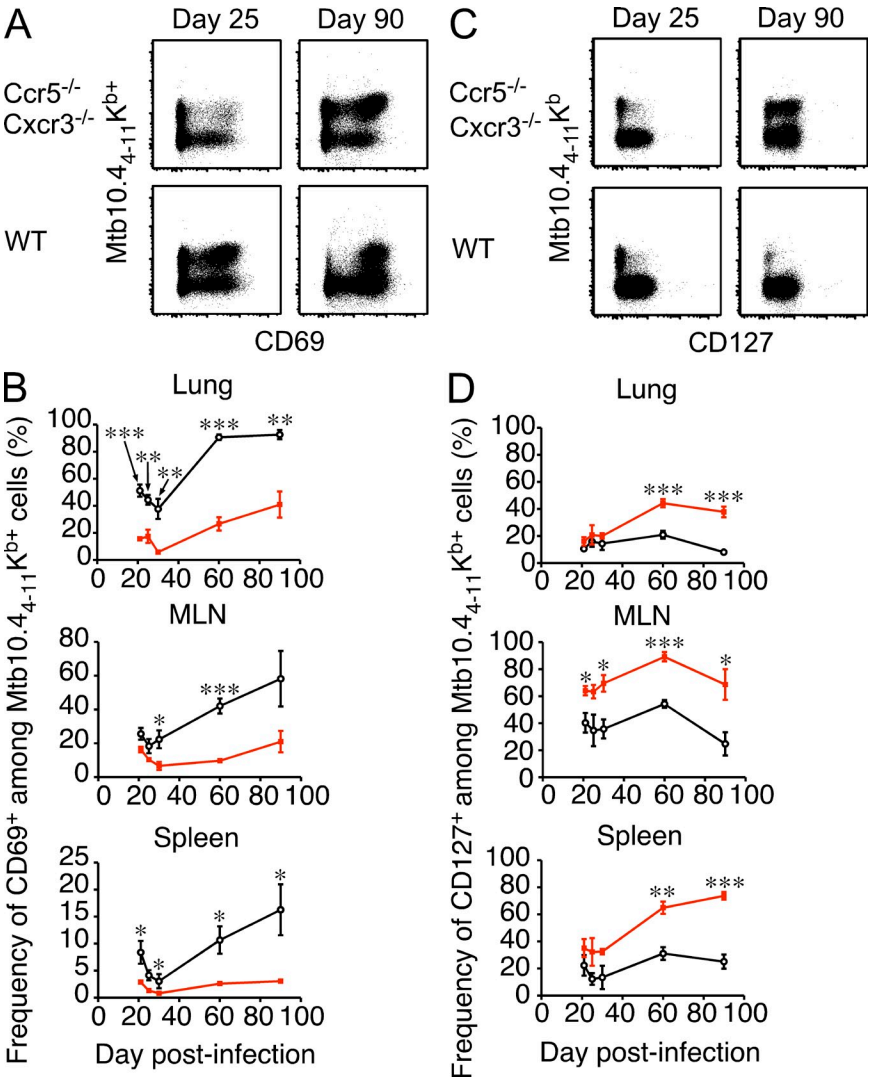

Figure 9. Mtb-specific *Ccr5*$^{-/-}$ *Cxcr3*$^{-/-}$ cells show decreased activation and enhanced CD127 expression during chronic infection. Mixed BM chimeras were infected with Mtb via the aerosol route and sacrificed at the indicated times. (A) Representative staining of Mtb10.4$_{4-11}$K^{b} tetramer and CD69 on *Ccr5*$^{-/-}$ *Cxcr3*$^{-/-}$ (top row) and WT (bottom row) cells in the lung on day 25 or 90 after infection. Plots are gated on CD8^{+} T cells. (B) The frequency of CD69^{+} WT (black) or *Ccr5*$^{-/-}$ *Cxcr3*$^{-/-}$ (red) Mtb-specific CD8^{+} T cells in the lung, MLN, and spleen at the indicated times after infection (mean ± SD; *, $P < 0.05$; **, $P < 0.005$; ***, $P < 0.0005$). (C) Representative staining of Mtb10.4$_{4-11}$K^{b} tetramer and CD127 on *Ccr5*$^{-/-}$ *Cxcr3*$^{-/-}$ (top row) and WT (bottom row) cells in the spleen on day 25 or 90 after infection. Plots are gated on CD8^{+} T cells. (D) The frequency of CD127^{+} WT (black) or *Ccr5*$^{-/-}$ *Cxcr3*$^{-/-}$ (red) Mtb-specific CD8^{+} T cells in the lung, MLN, and spleen at the indicated times after infection (mean ± SD; *, $P < 0.05$; **, $P < 0.005$; ***, $P < 0.0005$). The data are representative of two independent experiments with at least four mice per group.

the lung (Fig. 6 A), which supports our conclusion that chemokine-directed localization, rather than chemokine-mediated signals unrelated to cell migration, is responsible for the enhanced generation of T cell memory in our model. Our data clearly show that the decreased activation of influenza-specific T cells in the lung is primarily dependent on CXCR3, but not CCR5. Nevertheless, it is clear there is a considerable increase in the frequency and number of memory T cells in the absence of both CCR5 and CXCR3 when compared with CXCR3 alone (Fig. 1 and Fig. S2). As there is considerable redundancy in the chemokine system, it is possible that a role for CCR5 in memory T cell generation only becomes manifest in the absence of CXCR3. We are currently investigating this possibility to delineate the relative contributions of these two chemokine receptors in our model.

An especially intriguing finding is that even during chronic infection with Mtb, which is associated with high levels of persistent inflammation, antigen-specific *Ccr5*$^{-/-}$ *Cxcr3*$^{-/-}$ cells still display a quiescent, resting phenotype (Fig. 9). It has been previously shown that Mtb-specific memory CD8^{+} T cells do develop during the infection, and antibiotic clearance of the bacteria allows for effector CD8^{+} T cell contraction and the outgrowth of these Mtb-specific memory cells (Kamath et al., 2006). Similar to other chronic pathogens, Mtb-specific CD8^{+} T cells from patients show enhanced expression of programmed death 1, suggesting that these cells receive continual antigen stimulation (Jurado et al., 2008). In mice, the continual stimulation of CD8^{+} T cells during Mtb infection is suggested by the close association of CD8^{+} T cells with established granulomas in the lungs of chronically infected mice (Junqueira-Kipnis et al., 2004). It is possible that, similar to what we observed during influenza infection, *Ccr5*$^{-/-}$ *Cxcr3*$^{-/-}$ cells fail to migrate to the most inflamed areas, in this case the granuloma, and are therefore spared from chronic antigen encounter. This would explain both the lack of CD69 expression and the enhanced CD127 expression on *Ccr5*$^{-/-}$ *Cxcr3*$^{-/-}$ Mtb10.4$_{4-11}$K^{b}-specific CD8^{+} T cells, and we are currently investigating this possibility in more detail.

Because the ability of pathogen-specific CD8^{+} T cells to carry out their cytolytic functions depends on their ability to migrate to the infected site, the permanent inhibition of CCR5- and CXCR3-mediated signaling would likely be counter-productive to host fitness. Indeed, intact chemokine receptor–deficient mice are significantly more susceptible to PR8 influenza infection than WT mice (Fig. S1). However, our data suggest that temporarily inhibiting or dampening

these signals after vaccination may prove an effective technique for generating large numbers of robust memory T cells. Currently, there are several small molecule inhibitors directed against CCR5 and/or CXCR3 that have the potential to temporarily inhibit T cell migration during vaccination and may provide a means to increase vaccine efficacy (Proudfoot et al., 1996; Akashi et al., 2005; Rosenblum et al., 2009). For example, although peptide vaccination with a highly inflammatory adjuvant, such as complete Freund's adjuvant, usually generates memory $CD8^+$ T cells that show hallmarks of terminal differentiation and poor recall responses (Hikono et al., 2007), vaccinating while limiting the continual stimulation of antigen-specific T cells by inhibiting their migration to inflammatory chemokines may enhance both the number and quality of the T cell memory generated. This may be especially important for vaccination against certain pathogens, such as malaria, where abnormally high numbers of antigen-specific $CD8^+$ T cells are required for protection (Schmidt et al., 2008).

In conclusion, we describe a novel role for the inflammatory chemokine receptors CCR5 and CXCR3 in the generation of $CD8^+$ T cell memory. Pathogen-specific *Cxcr3*$^{-/-}$ and *Ccr5*$^{-/-}$ *Cxcr3*$^{-/-}$ cells are preferentially localized to noninflamed areas within infected tissues, which limits their ability to be reactivated by additional antigen encounters, resulting in greatly enhanced memory $CD8^+$ T cell generation. These data suggest that blocking T cell migration in response to CCR5 and CXCR3 ligands may enhance the generation of T cell memory after vaccination and temporarily inhibiting these chemokine receptors during chronic infection may enhance the quality of the antigen-specific memory T cell pool.

MATERIALS AND METHODS

Mice. Female C57BL/6J, B6.PL-Thy1a/Cy ($CD90.1^+$), B6.SJL-Ptprca Pep3/BoyJ ($CD45.1^+$), and B6.129P2-*Ccr5*^{tm1Kuz} /J (*Ccr5*$^{-/-}$) mice were purchased from The Jackson Laboratory. *Cxcr3*$^{-/-}$ and *Ccr5*$^{-/-}$ *Cxcr3*$^{-/-}$ double-deficient mice on the B6 background were generous gifts from C. Gerard (Harvard Medical School, Boston, MA) and A. Thomsen (University of Copenhagen, Copenhagen, Denmark), respectively (de Lemos et al., 2005; Hancock et al., 2000). Mixed BM chimeras were generated as previously described (Mayer et al., 2008) and allowed to reconstitute for 6 wk before infection. All animal studies were approved by the Trudeau Institute Animal Care and Use Committee.

Viruses, bacteria, and infections. Influenza viruses A/HK-x31 (x31, H3N2) and A/PR8 (PR8, H1N1) were grown, stored, and titered as previously described (Hou et al., 1992). Mtb strain H37Rv was grown and stored as previously described (Reiley et al., 2008). For influenza virus infection, mice were anesthetized with 2,2,2-tribromoethanol (200 mg/kg) and virus was administered intranasally (500 50% egg infectious doses [EID_{50}] for primary infections and 3×10^4 EID_{50} for secondary infections). For aerosol Mtb infection, animals were infected with a low dose (~75 CFU) of bacteria by using a Glas-Col airborne infection system.

Generation of BM-derived DCs. Single-cell suspensions of BM from C57BL/6J mice were cultured at 2×10^6 cells in RPMI containing 10% FCS, 100 U/ml penicillin and streptomycin, and 20 ng/ml of GM-CSF. Cultures were given fresh medium every 2–3 d, and incubated at 37°C for 10 d. On day 9, BM-derived DCs were resuspended in fresh medium containing 50 ng/ml LPS for 18 h to stimulate cells. For the last 3 h of culture, BM-derived DCs were pulsed with 10 μg/ml of $FluNP_{366\text{-}374}$ or γHV $p79_{524\text{-}531}$ peptide.

Tissue harvest and flow cytometry. Mice were sacrificed at the indicated times and tissues were harvested and processed as previously described (Kohlmeier et al., 2010). Single-cell suspensions were incubated with Fc-block (anti-CD16/32) for 15 min on ice, followed by staining with $FluNP_{366\text{-}374}D^b$ or $Mtb10.4_{4\text{-}11}K^b$ tetramers for 1 h at room temperature. Cells were then washed and stained with antibodies to CD8, CD44, CD45.1, CD45.2, CD69, and CD127 (eBioscience); CD8, CD27, CD62L, and CD69 (BD); CD43 (1B11), CD62L, and CD90.2 (BioLegend); and KLRG1 (SouthernBiotech). Samples were run on FACSCalibur, FACSCanto II, or LSR II flow cytometers (BD) and data were analyzed with FlowJo software (Tree Star).

Adoptive transfer and immunofluorescence microscopy. Mixed BM chimeras were infected with x31 influenza and rested for 45 d. WT, *Ccr5*$^{-/-}$, *Cxcr3*$^{-/-}$, and *Ccr5*$^{-/-}$ *Cxcr3*$^{-/-}$ effector memory T cells ($CD45.2^{+/-}$ $CD44^{hi}$ $CD62L^{lo}$) were sorted from the spleen. Sorting was performed on a FACSVantage cell sorter with DiVa electronics (BD). Aliquots of the sorted cells were stained with $FluNP_{366\text{-}374}D^b$ tetramer to determine the total number of FluNP-specific cells in each population, and the populations were mixed together such that the ratio of FluNP-specific WT and chemokine receptor–deficient cells was 1:1. This mixture was transferred i.v. into a congenic ($CD90.1^+$) host, and the host was infected with PR8 influenza 1 d later. On day 10 after infection, lungs were inflated with OCT (Sakura Finetek) and snap-frozen over liquid nitrogen. Frozen sections (7 μm) were fixed in acetone/ethanol and stained with antibodies against collagen type IV (R&D Systems), CD45.1-PE, and CD90.2-Alexa Fluor 647. Rabbit anti–mouse collagen type IV was detected with a goat anti–rabbit-Alexa Fluor 488 secondary antibody (Invitrogen). Staining was visualized with a Zeiss AxioVert 200M microscope using a 20× 0.75 na objective, and images were recorded with an AxioCam digital camera (Carl Zeiss, Inc.). Images were analyzed and converted to TIF files with AxioVision software (Carl Zeiss, Inc.).

Assessment of caspase activity. Caspase activity was assessed using the Vybrant FAM Poly Caspases Assay kit according to the manufacturer's instructions (Invitrogen). In brief, whole-lung homogenates were incubated at 37°C for 1 h in the presence of FAM-VAD-FMK poly caspases reagent. After incubation, cells were stained with tetramers and antibodies for flow cytometry as described above.

Measurement of BrdU uptake. Mice were administered BrdU (200 μl of a 4 mg/ml solution in PBS) i.p. and maintained on drinking water containing BrdU (0.8 mg/ml) for 24 h before harvest. Single-cell suspensions were stained with tetramers and antibodies to surface proteins as described above and BrdU incorporation was detected using the BrdU Flow kit (BD).

Measurement of virus titers. Whole-lung tissue was harvested in PBS at the indicated times, and lung homogenates were stored at −70°C. Virus titers were measured using a standard plaque assay by infecting MDCK cell monolayers with serial 10-fold dilutions of lung suspension in duplicate. 24 h after infection, monolayers were extensively washed and fixed with 80% acetone in water. Infected cell clusters were detected with a biotin-labeled mouse antiinfluenza A monoclonal antibody (Millipore), followed by staining with streptavidin-AP and visualized with Fast BCIP/NBT substrate (Sigma-Aldrich). The number of PFU were counted, and the data were shown as the PFU/lung (mean ± SD).

Histological analysis. Lungs were inflated with 5 ml neutral buffered formalin (10% vol/vol) via the trachea and fixed for 72 h. Lungs were embedded in paraffin wax, and 4–5-μm sections were mounted onto slides and stained with hematoxylin and eosin. The inflammatory score (on a scale of 0–4) was

assessed by a pathologist who was blinded as to the identity of the samples. All slides were viewed with an Axioplan 2 microscope and images were recorded with a Zeiss AxioCam digital camera (both from Carl Zeiss, Inc.).

Statistical analysis. Statistical analysis was performed using Prism 5 (GraphPad Software), and significance was determined by an unpaired two-tailed Student's *t* test. P-values less than 0.05 were considered significant.

Online supplemental material. Fig. S1 shows that *Ccr5*$^{-/-}$ *Cxcr3*$^{-/-}$ mice are highly susceptible to PR8 influenza infection. Fig. S2 shows that intact chemokine receptor–deficient mice have significantly larger numbers of memory T cells in the lung and spleen, and that these cells afford robust protection against lethal challenge. Fig. S3 shows that effector and memory *Ccr5*$^{-/-}$ *Cxcr3*$^{-/-}$ T cells are capable of producing cytokines and expressing granzyme B. Online supplemental material is available at http://www.jem.org/cgi/content/full/jem.20102110/DC1.

The authors thank the Trudeau Institute Molecular Biology Core for the production of MHC I tetramers, and Brandon Sells and Ron Lacourse for cell sorting.

This work was supported by National Institutes of Health grants AI067967, AI076499, and T32 AI049823 (D.L. Woodland), AI073564 (D.L. Woodland and G.M. Winslow), AI083610 (J.E. Kohlmeier), and funds from the Trudeau Institute.

The authors have no conflicting financial interests.

Submitted: 10 May 2010
Accepted: 21 June 2011

REFERENCES

Akashi, S., M. Sho, H. Kashizuka, K. Hamada, N. Ikeda, Y. Kuzumoto, Y. Tsurui, T. Nomi, T. Mizuno, H. Kanehiro, et al. 2005. A novel small-molecule compound targeting CCR5 and CXCR3 prevents acute and chronic allograft rejection. *Transplantation*. 80:378–384. doi:10.1097/01.tp.0000166338.99933.e1

Allan, R.S., J. Waithman, S. Bedoui, C.M. Jones, J.A. Villadangos, Y. Zhan, A.M. Lew, K. Shortman, W.R. Heath, and F.R. Carbone. 2006. Migratory dendritic cells transfer antigen to a lymph node-resident dendritic cell population for efficient CTL priming. *Immunity*. 25:153–162. doi:10.1016/j.immuni.2006.04.017

Badovinac, V.P., B.B. Porter, and J.T. Harty. 2002. Programmed contraction of CD8(+) T cells after infection. *Nat. Immunol.* 3:619–626. doi:10.1038/nrm880

Badovinac, V.P., K.A.N. Messingham, A. Jabbari, J.S. Haring, and J.T. Harty. 2005. Accelerated CD8+ T-cell memory and prime-boost response after dendritic-cell vaccination. *Nat. Med.* 11:748–756. doi:10.1038/nm1257

Bromley, S.K., T.R. Mempel, and A.D. Luster. 2008. Orchestrating the orchestrators: chemokines in control of T cell traffic. *Nat. Immunol.* 9:970–980. doi:10.1038/ni.f.213

Castellino, F., A.Y. Huang, G. Altan-Bonnet, S. Stoll, C. Scheinecker, and R.N. Germain. 2006. Chemokines enhance immunity by guiding naive CD8+ T cells to sites of CD4+ T cell-dendritic cell interaction. *Nature*. 440:890–895. doi:10.1038/nature04651

D'Cruz, L.M., M.P. Rubinstein, and A.W. Goldrath. 2009. Surviving the crash: transitioning from effector to memory CD8+ T cell. *Semin. Immunol.* 21:92–98. doi:10.1016/j.smim.2009.02.002

de Lemos, C., J.E. Christensen, A. Nansen, T. Moos, B. Lu, C. Gerard, J.P. Christensen, and A.R. Thomsen. 2005. Opposing effects of CXCR3 and CCR5 deficiency on CD8+ T cell-mediated inflammation in the central nervous system of virus-infected mice. *J. Immunol.* 175:1767–1775.

Dustin, M.L., S.K. Bromley, Z. Kan, D.A. Peterson, and E.R. Unanue. 1997. Antigen receptor engagement delivers a stop signal to migrating T lymphocytes. *Proc. Natl. Acad. Sci. USA*. 94:3909–3913. doi:10.1073/pnas.94.8.3909

Fadel, S.A., S.K. Bromley, B.D. Medoff, and A.D. Luster. 2008. CXCR3-deficiency protects influenza-infected CCR5-deficient mice from mortality. *Eur. J. Immunol.* 38:3376–3387. doi:10.1002/eji.200838628

Flynn, J.L. 2006. Lessons from experimental *Mycobacterium tuberculosis* infections. *Microbes Infect.* 8:1179–1188. doi:10.1016/j.micinf.2005.10.033

Galkina, E., J. Thatte, V. Dabak, M.B. Williams, K. Ley, and T.J. Braciale. 2005. Preferential migration of effector CD8+ T cells into the interstitium of the normal lung. *J. Clin. Invest.* 115:3473–3483. doi:10.1172/JCI24482

Hancock, W.W., B. Lu, W. Gao, V. Csizmadia, K. Faia, J.A. King, S.T. Smiley, M. Ling, N.P. Gerard, and C. Gerard. 2000. Requirement of the chemokine receptor CXCR3 for acute allograft rejection. *J. Exp. Med.* 192:1515–1520. doi:10.1084/jem.192.10.1515

Hand, T.W., M. Morre, and S.M. Kaech. 2007. Expression of IL-7 receptor alpha is necessary but not sufficient for the formation of memory CD8 T cells during viral infection. *Proc. Natl. Acad. Sci. USA*. 104:11730–11735. doi:10.1073/pnas.0705007104

Harty, J.T., and V.P. Badovinac. 2008. Shaping and reshaping CD8+ T-cell memory. *Nat. Rev. Immunol.* 8:107–119. doi:10.1038/nri2251

Hikono, H., J.E. Kohlmeier, S. Takamura, S.T. Wittmer, A.D. Roberts, and D.L. Woodland. 2007. Activation phenotype, rather than central- or effector-memory phenotype, predicts the recall efficacy of memory CD8$^+$ T cells. *J. Exp. Med.* 204:1625–1636. doi:10.1084/jem.20070322

Hou, S., P.C. Doherty, M. Zijlstra, R. Jaenisch, and J.M. Katz. 1992. Delayed clearance of Sendai virus in mice lacking class I MHC-restricted CD8+ T cells. *J. Immunol.* 149:1319–1325.

Huster, K.M., V. Busch, M. Schiemann, K. Linkemann, K.M. Kerksiek, H. Wagner, and D.H. Busch. 2004. Selective expression of IL-7 receptor on memory T cells identifies early CD40L-dependent generation of distinct CD8+ memory T cell subsets. *Proc. Natl. Acad. Sci. USA*. 101:5610–5615. doi:10.1073/pnas.0308054101

Jacobsen, M., A.K. Detjen, H. Mueller, A. Gutschmidt, S. Leitner, U. Wahn, K. Magdorf, and S.H. Kaufmann. 2007. Clonal expansion of CD8+ effector T cells in childhood tuberculosis. *J. Immunol.* 179:1331–1339.

Joshi, N.S., W. Cui, A. Chandele, H.K. Lee, D.R. Urso, J. Hagman, L. Gapin, and S.M. Kaech. 2007. Inflammation directs memory precursor and short-lived effector CD8(+) T cell fates via the graded expression of T-bet transcription factor. *Immunity*. 27:281–295. doi:10.1016/j.immuni.2007.07.010

Jung, Y.W., R.L. Rutishauser, N.S. Joshi, A.M. Haberman, and S.M. Kaech. 2010. Differential localization of effector and memory CD8 T cell subsets in lymphoid organs during acute viral infection. *J. Immunol.* 185:5315–5325. doi:10.4049/jimmunol.1001948

Junqueira-Kipnis, A.P., J. Turner, M. Gonzalez-Juarrero, O.C. Turner, and I.M. Orme. 2004. Stable T-cell population expressing an effector cell surface phenotype in the lungs of mice chronically infected with *Mycobacterium tuberculosis*. *Infect. Immun.* 72:570–575. doi:10.1128/IAI.72.1.570-575.2004

Jurado, J.O., I.B. Alvarez, V. Pasquinelli, G.J. Martínez, M.F. Quiroga, E. Abbate, R.M. Musella, H.E. Chuluyan, and V.E. García. 2008. Programmed death (PD)-1:PD-ligand 1/PD-ligand 2 pathway inhibits T cell effector functions during human tuberculosis. *J. Immunol.* 181:116–125.

Kaech, S.M., and E.J. Wherry. 2007. Heterogeneity and cell-fate decisions in effector and memory CD8+ T cell differentiation during viral infection. *Immunity*. 27:393–405. doi:10.1016/j.immuni.2007.08.007

Kaech, S.M., J.T. Tan, E.J. Wherry, B.T. Konieczny, C.D. Surh, and R. Ahmed. 2003. Selective expression of the interleukin 7 receptor identifies effector CD8 T cells that give rise to long-lived memory cells. *Nat. Immunol.* 4:1191–1198. doi:10.1038/ni1009

Kamath, A., J.S. Woodworth, and S.M. Behar. 2006. Antigen-specific CD8+ T cells and the development of central memory during *Mycobacterium tuberculosis* infection. *J. Immunol.* 177:6361–6369.

Kedzierska, K., N.L. La Gruta, S.J. Turner, and P.C. Doherty. 2006. Establishment and recall of CD8+ T-cell memory in a model of localized transient infection. *Immunol. Rev.* 211:133–145. doi:10.1111/j.0105-2896.2006.00386.x

Kohlmeier, J.E., and D.L. Woodland. 2009. Immunity to respiratory viruses. *Annu. Rev. Immunol.* 27:61–82. doi:10.1146/annurev.immunol.021908.132625

Kohlmeier, J.E., S.C. Miller, J. Smith, B. Lu, C. Gerard, T. Cookenham, A.D. Roberts, and D.L. Woodland. 2008. The chemokine receptor

CCR5 plays a key role in the early memory CD8+ T cell response to respiratory virus infections. *Immunity*. 29:101–113. doi:10.1016/j.immuni.2008.05.011

Kohlmeier, J.E., T. Cookenham, S.C. Miller, A.D. Roberts, J.P. Christensen, A.R. Thomsen, and D.L. Woodland. 2009. CXCR3 directs antigen-specific effector CD4+ T cell migration to the lung during parainfluenza virus infection. *J. Immunol.* 183:4378–4384. doi:10.4049/jimmunol.0902022

Kohlmeier, J.E., T. Cookenham, A.D. Roberts, S.C. Miller, and D.L. Woodland. 2010. Type I interferons regulate cytolytic activity of memory CD8(+) T cells in the lung airways during respiratory virus challenge. *Immunity*. 33:96–105. doi:10.1016/j.immuni.2010.06.016

Kolumam, G.A., S. Thomas, L.J. Thompson, J. Sprent, and K. Murali-Krishna. 2005. Type I interferons act directly on CD8 T cells to allow clonal expansion and memory formation in response to viral infection. *J. Exp. Med.* 202:637–650. doi:10.1084/jem.20050821

Lawrence, C.W., and T.J. Braciale. 2004. Activation, differentiation, and migration of naive virus-specific CD8+ T cells during pulmonary influenza virus infection. *J. Immunol.* 173:1209–1218.

Legge, K.L., and T.J. Braciale. 2003. Accelerated migration of respiratory dendritic cells to the regional lymph nodes is limited to the early phase of pulmonary infection. *Immunity*. 18:265–277. doi:10.1016/S1074-7613(03)00023-2

Lindell, D.M., T.E. Lane, and N.W. Lukacs. 2008. CXCL10/CXCR3-mediated responses promote immunity to respiratory syncytial virus infection by augmenting dendritic cell and CD8(+) T cell efficacy. *Eur. J. Immunol.* 38:2168–2179. doi:10.1002/eji.200838155

Mayer, K.D., K. Mohrs, W. Reiley, S. Wittmer, J.E. Kohlmeier, J.E. Pearl, A.M. Cooper, L.L. Johnson, D.L. Woodland, and M. Mohrs. 2008. Cutting edge: T-bet and IL-27R are critical for in vivo IFN-gamma production by CD8 T cells during infection. *J. Immunol.* 180:693–697.

McGill, J., and K.L. Legge. 2009. Cutting edge: contribution of lung-resident T cell proliferation to the overall magnitude of the antigen-specific CD8 T cell response in the lungs following murine influenza virus infection. *J. Immunol.* 183:4177–4181. doi:10.4049/jimmunol.0901109

McGill, J., N. Van Rooijen, and K.L. Legge. 2010. IL-15 trans-presentation by pulmonary dendritic cells promotes effector CD8 T cell survival during influenza virus infection. *J. Exp. Med.* 207:521–534. doi:10.1084/jem.20091711

Newton, P., G. O'Boyle, Y. Jenkins, S. Ali, and J.A. Kirby. 2009. T cell extravasation: demonstration of synergy between activation of CXCR3 and the T cell receptor. *Mol. Immunol.* 47:485–492. doi:10.1016/j.molimm.2009.08.021

Obar, J.J., and L. Lefrançois. 2010. Early events governing memory CD8+ T-cell differentiation. *Int. Immunol.* 22:619–625. doi:10.1093/intimm/dxq053

Pearce, E.L., and H. Shen. 2007. Generation of CD8 T cell memory is regulated by IL-12. *J. Immunol.* 179:2074–2081.

Prlic, M., and M.J. Bevan. 2008. Exploring regulatory mechanisms of CD8+ T cell contraction. *Proc. Natl. Acad. Sci. USA*. 105:16689–16694. doi:10.1073/pnas.0808997105

Proudfoot, A.E., C.A. Power, A.J. Hoogewerf, M.O. Montjovent, F. Borlat, R.E. Offord, and T.N. Wells. 1996. Extension of recombinant human RANTES by the retention of the initiating methionine produces a potent antagonist. *J. Biol. Chem.* 271:2599–2603. doi:10.1074/jbc.271.5.2599

Redmond, W.L., and L.A. Sherman. 2005. Peripheral tolerance of CD8 T lymphocytes. *Immunity*. 22:275–284. doi:10.1016/j.immuni.2005.01.010

Reiley, W.W., M.D. Calayag, S.T. Wittmer, J.L. Huntington, J.E. Pearl, J.J. Fountain, C.A. Martino, A.D. Roberts, A.M. Cooper, G.M. Winslow, and D.L. Woodland. 2008. ESAT-6-specific CD4 T cell responses to aerosol *Mycobacterium tuberculosis* infection are initiated in the mediastinal lymph nodes. *Proc. Natl. Acad. Sci. USA*. 105:10961–10966. doi:10.1073/pnas.0801496105

Rosenblum, J.M., Q.W. Zhang, G. Siu, T.L. Collins, T. Sullivan, D.J. Dairaghi, J.C. Medina, and R.L. Fairchild. 2009. CXCR3 antagonism impairs the development of donor-reactive, IFN-gamma-producing effectors and prolongs allograft survival. *Transplantation*. 87:360–369. doi:10.1097/TP.0b013e31819574e9

Rosenblum, J.M., N. Shimoda, A.D. Schenk, H. Zhang, D.D. Kish, K. Keslar, J.M. Farber, and R.L. Fairchild. 2010. CXC chemokine ligand (CXCL) 9 and CXCL10 are antagonistic costimulation molecules during the priming of alloreactive T cell effectors. *J. Immunol.* 184:3450–3460. doi:10.4049/jimmunol.0903831

Rubinstein, M.P., N.A. Lind, J.F. Purton, P. Filippou, J.A. Best, P.A. McGhee, C.D. Surh, and A.W. Goldrath. 2008. IL-7 and IL-15 differentially regulate CD8+ T-cell subsets during contraction of the immune response. *Blood*. 112:3704–3712. doi:10.1182/blood-2008-06-160945

Sandau, M.M., J.E. Kohlmeier, D.L. Woodland, and S.C. Jameson. 2010. IL-15 regulates both quantitative and qualitative features of the memory CD8 T cell pool. *J. Immunol.* 184:35–44. doi:10.4049/jimmunol.0803355

Schluns, K.S., W.C. Kieper, S.C. Jameson, and L. Lefrançois. 2000. Interleukin-7 mediates the homeostasis of naïve and memory CD8 T cells in vivo. *Nat. Immunol.* 1:426–432. doi:10.1038/80868

Schmidt, N.W., R.L. Podyminogin, N.S. Butler, V.P. Badovinac, B.J. Tucker, K.S. Bahjat, P. Lauer, A. Reyes-Sandoval, C.L. Hutchings, A.C. Moore, et al. 2008. Memory CD8 T cell responses exceeding a large but definable threshold provide long-term immunity to malaria. *Proc. Natl. Acad. Sci. USA*. 105:14017–14022. doi:10.1073/pnas.0805452105

Schwarz, J.B., N. Langwieser, N.N. Langwieser, M.J. Bek, S. Seidl, H.H. Eckstein, B. Lu, A. Schomig, H. Pavenstadt, and D. Zohlnhofer. 2009. Novel role of the CXC chemokine receptor 3 in inflammatory response to arterial injury: involvement of mTORC1. *Circ Res* 104:189-200, 188p following 200.

Semmling, V., V. Lukacs-Kornek, C.A. Thaiss, T. Quast, K. Hochheiser, U. Panzer, J. Rossjohn, P. Perlmutter, J. Cao, D.I. Godfrey, et al. 2010. Alternative cross-priming through CCL17-CCR4-mediated attraction of CTLs toward NKT cell-licensed DCs. *Nat. Immunol.* 11:313–320. doi:10.1038/ni.1848

Shin, H., and E.J. Wherry. 2007. CD8 T cell dysfunction during chronic viral infection. *Curr. Opin. Immunol.* 19:408–415. doi:10.1016/j.coi.2007.06.004

Shiow, L.R., D.B. Rosen, N. Brdicková, Y. Xu, J. An, L.L. Lanier, J.G. Cyster, and M. Matloubian. 2006. CD69 acts downstream of interferon-alpha/beta to inhibit S1P1 and lymphocyte egress from lymphoid organs. *Nature*. 440:540–544. doi:10.1038/nature04606

Strasser, A., and M. Pellegrini. 2004. T-lymphocyte death during shutdown of an immune response. *Trends Immunol.* 25:610–615. doi:10.1016/j.it.2004.08.012

Williams, M.A., and M.J. Bevan. 2007. Effector and memory CTL differentiation. *Annu. Rev. Immunol.* 25:171–192. doi:10.1146/annurev.immunol.25.022106.141548